HEATING A PLASMA BY A BROADBAND STREAM OF FAST ELECTRONS: FAST IGNITION, SHOCK IGNITION, AND Gbar SHOCK WAVE APPLICATIONS

S. Yu. Gus'kov [a,b*], *Ph. Nicolai* [c], *X. Ribeyre* [c], *V. T. Tikhonchuk* [c]

[a] *Lebedev Physical Institute, Russian Academy of Sciences*
119991, Moscow, Russia

[b] *National Research Nuclear University "MEPhI"*
115409, Moscow, Russia

[c] *University of Bordeaux-CNRS-CEA, Centre Lasers Intenses et Applications*
33405, Talence, France

An exact analytic solution is found for the steady-state distribution function of fast electrons with an arbitrary initial spectrum irradiating a planar low-Z plasma with an arbitrary density distribution. The solution is applied to study the heating of a material by fast electrons of different spectra such as a monoenergetic spectrum, a step-like distribution in a given energy range, and a Maxwellian spectrum, which is inherent to laser-produced fast electrons. The heating of shock- and fast-ignited precompressed inertial confinement fusion (ICF) targets as well as the heating of a target designed to generate a Gbar shock wave for EOS experiments by laser-produced fast electrons with a Maxwellian spectrum is investigated. A relation is established between the energies of two groups of Maxwellian fast electrons, which are responsible for generation of a shock wave and heating the upstream material (preheating). The minimum energy of the fast and shock igniting beams as well as of the beam for a Gbar shock wave generation increases with the spectral width of the electron distribution.

1. INTRODUCTION

Interaction of an intense beam of charged particles with plasma is an essential part of the modern high-energy-density physics. The development of the kinetic theory of such interaction is important primarily for the studies of a powerful laser pulse interaction with matter and the equation of state (EOS) of matter under extreme conditions. Generation of fast electrons and ions is one of the most interesting and important phenomena of the intense laser radiation interaction with matter. Generation of fast electrons is due to different mechanisms associated with the resonant absorption of laser radiation at the critical-density plasma [1], the Brunel effect [2], the ponderomotive force [3], and the development of various plasma instabilities [4]. Acceleration of fast ions occurs both directly, as a result of the ponderomotive pressure of laser radiation, and in-

directly, in a self-consistent field of fast electrons. Speaking about laser-accelerated fast electrons, we note that the characteristic fast electron energy for all the generation mechanisms is comparable with the average energy of electron oscillations in a laser field. This last energy is proportional to the coupling parameter $I\lambda^2$ (where I and λ are respectively the intensity and the wavelength of radiation). In the current experiments using petawatt lasers, the average fast electron energy exceeds 1 MeV and the efficiency of laser energy conversion into fast electrons is about 30 % (see, e. g., reviews [5, 6]). The spectrum of the laser-accelerated fast electrons is usually close to the Maxwellian distribution.

The transfer of a fraction of the absorbed laser energy in a dense region of a laser-irradiated target (with a density higher than the critical plasma density) by fast electrons can play a much greater role than the heating due to an electron thermal conductivity wave. The energy transfer by fast electrons plays a dominant role if the coupling parameter ex-

*E-mail: guskov@sci.lebedev.ru

ceeds 1–10 PW·μm^2/cm^2 [7,8], while the energy transfer by electron thermal conductivity is strongly inhibited. Heating the precompressed plasma to a thermonuclear temperature by laser-produced fast electrons is one of the promising methods of the fast ignition concept [9, 10] in inertial confinement fusion (ICF). Generation of a powerful shock wave due to the transfer of the absorbed laser energy by fast electrons is a key element in another promising method of ICF target ignition, the shock ignition [11, 12]. It has been shown [13] that the shock wave with a pressure of 0.4–2 Gbar can be generated when a solid target is irradiated by a fast electron beam with an energy of 30–100 keV, corresponding to the laser pulse intensity 10–100 PW/cm^2. Such a shock wave exists in the time interval of 0.3–1 ns and it is able to provide the shock ignition of an ICF target. Besides, the application of shock wave generation in a solid by a fast electron beam opens a possibility to step out from the current level of ablation pressure of 100 Mbar to a new level of several hundred Mbar or even Gbar in laboratory EOS studies.

In this context, an important question is the role of the initial spectrum of fast electrons. In the fast ignition of a compressed ICF target, the fast electron spectrum determines the spatial distribution of the plasma temperature in the ignition region and consequently the heated mass. In the shock ignition, the fast electron spectrum determines the position of the ablation front and preheating of the material ahead of the shock-wave. The conventional approach in the high-pressure hydrodynamics of laser-produced plasma is traditionally limited to the values of coupling parameter $I\lambda^2$ below 0.1 PW·μm^2/cm^2 [14, 15] in order to avoid the fast electron preheating. This was a baseline argument for using a short-wavelength laser radiation, in particular, the radiation of the third harmonic of Nd-lasers ($\lambda = 0.353$ μm) in ICF.

The experiments in [16] on the irradiation of spherical targets by long wavelength radiation of a CO_2-laser ($\lambda = 10.6$ μm) with the intensity $I = 0.01$–0.1 PW/cm^2 (with the coupling parameter about 10–100 PW·μm^2/cm^2) and accompanying theoretical studies carried out in the early 1980s were of great importance for understanding the role of fast electrons. The influence of the laser-produced fast electron preheating on the reduction of target compression [17] as well as the positive role of energy transfer by fast electrons in increasing the ablation pressure [18] were reported. The matching conditions that relate the shell thickness of the ICF target and the laser pulse parameters have been proposed [19]. They define the conditions under which the fast electron preheating of a compressed thermonuclear fuel can be suppressed with a significant contribution of the fast electron energy transfer to the ablation pressure formation. Such a matching is a basis for the modern concept of shock ignition. Both numerical simulations and analytic models are used for studying laser-produced fast electron transport in the targets of various geometries. Such models have been constructed in [18, 20] based on an analytic solution of the kinetic equation in spherical geometry for fast electrons having a monoenergetic spectrum. A model of stopping of fast electrons with a Maxwellian spectrum in a planar plasma layer based on an analytic approximation of the results of numerical calculations was developed in [21].

The theory of fast electron kinetics is developed in this paper for an arbitrary electron spectrum in planar geometry. An exact analytic solution of a steady-state relativistic kinetic equation for the distribution function of fast electrons is found and used to develop the model of heating a plain target. An analytic solution for the spatial distribution of the fast electron energy deposited in a plasma and hence for the spatial distribution of the temperature in the heated region is obtained. The heating of a shock- and fast-ignited precompressed ICF targets by laser-produced fast electrons is investigated. A criterion for the generation of a shock wave is obtained in the case of a decreasing temperature (pressure) profile of matter heated by fast electrons of a Maxwellian spectrum, which is the most common for laser-accelerated particles. By using such a criterion, the fractions of fast electron energy spent for ablation of the target material and preheating the material ahead of the shock front are found. The laser pulse parameters are derived that allow generating a shock wave for laboratory investigation of the EOS of materials on the Gbar level of pressure. The temperature profile in the ignition region of a fast-ignited ICF target is found and the minimal energy of the fast electron beam with a Maxwellian spectrum needed for ignition is calculated.

The results of the studies are presented as follows. In Sec. 2, a solution of the relativistic kinetic equation for fast electrons with an arbitrary spectrum is presented. In Sec. 3, in the particular cases of nonrelativistic and ultra-relativistic fast electrons, analytic solutions for the distribution function and the deposited energy spatial distribution are presented for several types of the initial spectrum, including the Maxwellian one. Section 4 is devoted to the applications related to the fast electron heating of shock- and fast-ignited ICF targets as well as to the Gbar shock wave generation for EOS studies.

2. EXACT SOLUTION OF THE STEADY-STATE KINETIC EQUATION FOR STOPPING FAST ELECTRONS HAVING AN ARBITRARY INITIAL SPECTRUM

We consider a dense semi-space plasma of low-Z materials, such as DT and light materials of an ICF target ablator such as plastic or beryllium heated by a fast electron bunch with an arbitrary energy distribution. We are interested in a sufficiently long bunch with a duration of several tens of ps and more, consisting of electrons with the average energy larger than several keV. Under these conditions, the time of fast electron slowing down is a fraction of a ps and the angle of scattering is less than $10°$. That allows studying the problem in the steady-state approximation and considering the stopping of fast electron along a straight trajectory, taking a small correction for scattering by reducing the fast electron range into account.

The statement of the steady-state kinetic problem for the distribution function of relativistic electrons incident on a planar semi-space boundary ($x = 0$) along the normal and decelerating there, consists of the kinetic equation (see, e. g., [20])

$$\frac{p}{\gamma m_e}\frac{\partial f}{\partial x} + \frac{\partial g\, f}{\partial p} = 0 \qquad (1)$$

together with the boundary condition

$$f|_{x=0} = n_b S(p), \qquad (2)$$

where f is the distribution function of fast electrons in the phase space, with the momentum p and the spatial coordinate x; n_b and $S(p)$ are the density and spectrum of fast electrons on the boundary of the heated semi-space;

$$\gamma = \left(1 + \frac{p^2}{m_e^2 c^2}\right)^{1/2};$$

c is the speed of light, m_e is the electron rest mass, and $g = dp/dt$ is the fast electron stopping rate, which is described by the expressions

$$g = -g_0\rho\frac{\gamma^2}{p^2}, \quad g_0 = \frac{4\pi e^4 Z m_e}{A m_p}\ln\Lambda, \qquad (3)$$

e and m_p are the electron charge and the proton mass; Z and A are the ion charge and atomic number; ρ is the plasma mass density, and $\ln\Lambda$ is the Coulomb logarithm.

The equation implies the equality of the kinetic energy introduced in the semi-space by a fast electron and the energy deposited there:

$$\int n_b S(p) E\, dp \equiv \int n_b S(p) m_e c^2 \times$$
$$\times \left[\left(1 + \frac{p^2}{m_e^2 c^2}\right)^{1/2} - 1\right] dp = \int W\, dx, \qquad (4)$$

where W is the specific heating rate, that is, the fast-electron energy deposited in a unit volume of the semi-space per unit time,

$$W \equiv \int f\frac{dE}{dt}\, dp = \frac{\rho(x)g_0}{m_e^2 c}\int f\left(\frac{m_e^2 c^2 + p^2}{p^2}\right)^{1/2} dp, \qquad (5)$$

E is the kinetic energy of the fast electron,

$$E = \left(p^2 c^2 + m_e^2 c^4\right)^{1/2} - m_e c^2 = m_e c^2(\gamma - 1),$$

and

$$\frac{dE}{dt} = \frac{p}{\gamma m_e}\frac{dp}{dt}.$$

Introducing the new variables

$$m = \int_{x'}^{x}\rho\, dx \quad \text{and}$$
$$\mu = \int_{p'}^{p}\frac{p^3}{m_e g_0\left(1 + \dfrac{p^2}{m_e^2 c^2}\right)^{3/2}}\, dp \qquad (6)$$

we rewrite Eq. (1) as

$$\frac{dF}{d\xi} = 0, \qquad (7)$$

where

$$F = f\frac{p^2 + m_e^2 c^2}{p^2 m_e^2 c^2} \quad \text{and} \quad \xi = m + \mu.$$

Then the solution for the fast electron distribution function satisfying boundary condition (2) is

$$f = n_b S(p')\frac{p^2}{p'^2}\frac{p'^2 + m_e^2 c^2}{p^2 + m_e^2 c^2}, \qquad (8)$$

where the momentum p' that the fast electron has on the boundary of the semi-space at the coordinate $x = 0$, and the momentum p that the same fast electron has at the semi-space point with the current coordinate x ($p \le p'$) are determined by

$$\int_0^x \rho\, dx = \int_p^{p'}\frac{p^3}{m_e g_0\left(1 + \dfrac{p^2}{m_e^2 c^2}\right)^{3/2}}\, dp. \qquad (9)$$

Performing the integration in (9) yields an exact expression for the stopping range μ of the fast electron,

where its momentum decreases from p' to p, in the general relativistic case

$$\mu = \mu_0 \left[1 - \frac{\gamma(p')}{\gamma(p)} \left(\frac{\gamma(p)-1}{\gamma(p')-1} \right)^2 \right], \qquad (10)$$

where μ_0 is the total stopping range of the fast electron decelerated from an arbitrary momentum $p = p'$ to $p = 0$

$$m_0 = \frac{m_e^3 c^4}{g_0} \frac{[\gamma(p')-1]^2}{\gamma(p')}. \qquad (11)$$

Expression (11) is exact, in contrast to Refs. [10, 13, 22], where approximate expressions were used to determine the total range of a fast electron for both nonrelativistic and relativistic cases. From (10), we obtain an explicit expression that connects the values of p' and p via the mass m corresponding to the distance crossed by a fast electron:

$$p' = \frac{m_e c}{2} \left\{ \left[(a+2) + \left((a+2)^2 - 4 \right)^{1/2} \right]^2 - 4 \right\}^{1/2}, \quad (12)$$

where

$$a = \frac{[\gamma(p)-1]^2}{\gamma(p)} + \frac{mg_0}{m_e^3 c^4} \equiv$$

$$\equiv \frac{\left[\left(1 + \dfrac{p^2}{m_e^2 c^2} \right)^{1/2} - 1 \right]^2}{\left(1 + \dfrac{p^2}{m_e^2 c^2} \right)^{1/2}} + \frac{mg_0}{m_e^3 c^4} \quad (13)$$

and

$$m = \int\limits_0^x \rho \, dx. \qquad (14)$$

Expressions (8), (12), and (13) analytically determine the distribution function of fast electrons in a nonuniform plasma semi-space with an arbitrary spectrum at the boundary.

The specific heating rate W, according to (5), can be calculated using solution (8) as

$$W \equiv \int f \frac{dE}{dt} \, dp = \frac{\rho(x) g_0 n_b}{m_e^2 c} \times$$

$$\times \int \frac{S(p') \left(1 + \dfrac{m_e^2 c^2}{p'^2} \right)}{\left(1 + \dfrac{m_e^2 c^2}{p^2} \right)^{1/2}} \, dp. \quad (15)$$

Here, the values p' and p are related by (12) with (13) and (14) taken into account. The specific heating rate determines the growth rate of the plasma temperature

T_p in the semi-space region heated by fast electrons (assuming the electron–ion relaxation, we suppose that $T_e = T_i = T_p$)

$$\frac{dT_p}{dt} = \frac{W}{C_V \rho}, \qquad (16)$$

where

$$C_V = \frac{(Z+1)k_B}{A(\gamma_a + 1)m_i}$$

is the specific heat, k_B is the Boltzmann constant, γ_a is the adiabatic exponent, and m_i is the mass of plasma ions.

3. HEATING OF PLASMA BY FAST ELECTRONS WITH DIFFERENT INITIAL ENERGY DISTRIBUTIONS

We consider the heating a plasma semi-space by a stream of fast electrons with different initial spectra, namely, a monoenergetic, a step-like, and a Maxwellian one. The last spectrum is the most relevant to laser-produced fast electrons. We discuss results for both nonrelativistic and ultra-relativistic fast electrons, which are described by simple expressions. The results for the ultra-relativistic case are obtained under the approximation that the fast electrons transfer practically all of their energy, but remain relativistic. Besides, for simplicity in the ultra-relativistic case, the electron rest energy is neglected. Also, to simplify the presentation, we consider a homogeneous plasma.

According to (3), the stopping power of nonrelativistic fast electrons is given by

$$g = -\frac{g_0 \rho}{p^2}, \quad \frac{dE}{dt} = \frac{pg}{m_e}, \qquad (17)$$

where $p = m_e v$ and $p = (2Em_e)^{1/2}$. Accordingly, the stopping length of a nonrelativistic fast electron that decelerates from the initial momentum p_0 to the final momentum $p = 0$ is obtained from the general expression (11) as

$$\lambda_0 = \frac{p_0^4}{4g_0 \rho_0 m_e}. \qquad (18)$$

In the case of ultra-relativistic fast electrons, these values are equal to

$$g = -\frac{g_0 \rho}{m_e^2 c^2}, \quad \frac{dE}{dt} = cg, \qquad (19)$$

$$\lambda_0 = \frac{(m_e c)^3 p_0}{g_0 \rho_0 m_e}, \qquad (20)$$

where $p = E/c$.

3.1. Monoenergetic spectrum

For the initial spectrum of fast electrons

$$S(p') = \delta(p' - p_0),$$

the distribution functions for nonrelativistic and ultra-relativistic fast electrons are respectively given by

$$f(x, \nu) = n_b \delta \left[\left(p^4 + p_0^4 \frac{x}{\lambda_0} \right)^{1/4} - p_0 \right] \times$$

$$\times \left[1 + \left(\frac{p_0}{p} \right)^4 \frac{x}{\lambda_0} \right]^{-1/2}$$

and

$$f(x, \nu) = n_b \delta \left[\left(p + p_0 \frac{x}{\lambda_0} \right) - p_0 \right].$$

Performing the integration in accordance with (5), we obtain the following expressions for specific heating in the respective cases of nonrelativistic and ultra-relativistic fast electrons:

$$W = \frac{q_0}{2\lambda_0} \left(1 - \frac{x}{\lambda_0} \right)^{-1/2}, \quad 0 \le x \le \lambda_0;$$
$$q_0 = n_b \frac{p_0^3}{2m_e^2} \tag{21}$$

and

$$W = \frac{q_0}{\lambda_0}, \quad 0 \le x \le \lambda_0; \quad q_0 = n_b p_0 c^2, \tag{22}$$

where q_0 is the energy flux of fast electrons at the boundary and the stopping lengths of nonrelativistic and ultra-relativistic fast electron are given by expressions (18) and (20).

The energy transmitted to the plasma layer of a thickness x per unit time — the layer heating power — in the respective cases of nonrelativistic and ultra-relativistic fast electrons is

$$q \equiv \int_0^x W(x') \, dx' = q_0 \left[1 - \left(1 - \frac{x}{\lambda_0} \right)^{1/2} \right], \tag{23}$$

$$0 \le x \le \lambda_0,$$

and

$$q = q_0 \frac{x}{\lambda_0}. \tag{24}$$

3.2. Step-like spectrum

For the initial spectrum of fast electrons in the form

$$S(p') = \begin{cases} (\Delta p)^{-1}, & p_{min} \le p' \le p_{max}, \\ \\ 0, & p' < p_{min}, \quad p' > p_{max}, \end{cases}$$

where $\Delta p = p_{max} - p_{min}$, the respective distribution functions for nonrelativistic and ultra-relativistic fast electrons are

$$f(x, p) = \frac{n_b}{\Delta p} \left(1 + \frac{x}{\lambda(p)} \right)^{-1/2}, \tag{25}$$

where

$$\lambda(p) = \frac{p^4}{4g_0 \rho m_e}, \quad \lambda_{min} - x \le \lambda(p) \le \lambda_{max} - x, \tag{26}$$

$$\lambda_{min} = \frac{p_{min}^4}{4g_0 \rho m_e}, \quad \lambda_{max} = \frac{p_{max}^4}{4g_0 \rho m_e},$$

and

$$f(x, p) = \frac{n_b}{\Delta p}, \tag{27}$$

where

$$\lambda_{min} - x \le \lambda(p) \le \lambda_{max} - x, \tag{28}$$

$$\lambda(p) = \frac{(m_e c)^3 p}{g_0 \rho m_e},$$

$$\lambda_{min} = \frac{(m_e c)^3 p_{min}}{g_0 \rho m_e}, \quad \lambda_{max} = \frac{(m_e c)^3 p_{max}}{g_0 \rho m_e}.$$

Then the specific heating rate and the energy transmitted to the boundary layer per unit time by a nonrelativistic fast electron stream with a step-like spectrum are

$$W(x) = \frac{q_0}{\lambda_{max} - \lambda_{min}} \begin{cases} \ln \left\{ \left(\frac{\lambda_{max}}{\lambda_{min}} \right)^{1/2} \left[\frac{1 + (1 - x/\lambda_{max})^{1/2}}{1 + (1 - x/\lambda_{min})^{1/2}} \right] \right\}, & 0 \le x \le \lambda_{min}, \\ \\ \ln \left\{ \left(\frac{\lambda_{max}}{x} \right)^{1/2} \left[1 + \left(1 - \frac{x}{\lambda_{max}} \right)^{1/2} \right] \right\}, & \lambda_{min} \le x \le \lambda_{max}, \end{cases} \tag{29}$$

$$q(x) = \frac{q_0}{\lambda_{max} - \lambda_{min}} \times$$

$$\times \begin{cases} \lambda_{max} \left[1 - \left(1 - \frac{x}{\lambda_{max}} \right)^{1/2} \right] - \lambda_{min} \left[1 - \left(1 - \frac{x}{\lambda_{min}} \right)^{1/2} \right] + \\ + x \ln \left\{ \left(\frac{\lambda_{max}}{\lambda_{min}} \right)^{1/2} \frac{1 + (1 - x/\lambda_{max})^{1/2}}{1 + (1 - x/\lambda_{min})^{1/2}} \right\}, \qquad 0 \le x \le \lambda_{min}, \\ (\lambda_{max} - \lambda_{min}) - \lambda_{max} \left(1 - \frac{x}{\lambda_{max}} \right)^{1/2} + \\ + x \ln \left\{ \left(\frac{\lambda_{max}}{x} \right)^{1/2} \left[1 + \left(1 - \frac{x}{\lambda_{max}} \right)^{1/2} \right] \right\}, \qquad \lambda_{min} \le x \le \lambda_{max}, \end{cases} \tag{30}$$

where the energy flux carried by the fast electron stream is given by

$$q_0 = \frac{n_b}{8m_e^2} (p_{max} + p_{min}) \left(p_{max}^2 + p_{min}^2 \right).$$

For an ultra-relativistic fast electron stream with a step-like spectrum, we obtain

$$W(x) = \frac{2q_0 \lambda_{max}}{\lambda_{max}^2 - \lambda_{min}^2} \times$$

$$\times \begin{cases} 1 - \frac{\lambda_{min}}{\lambda_{max}}, & 0 \le x \le \lambda_{min}, \\ 1 - \frac{x}{\lambda_{max}}, & \lambda_{min} \le x \le \lambda_{max}, \end{cases} \tag{31}$$

$$q(x) = \frac{2q_0 \lambda_{max}}{\lambda_{max}^2 - \lambda_{min}^2} \times$$

$$\times \begin{cases} \left(1 - \frac{\lambda_{min}}{\lambda_{max}} \right) x, & 0 \le x \le \lambda_{min}, \\ x - \frac{x^2 + \lambda_{min}^2}{2\lambda_{max}}, & \lambda_{min} \le x \le \lambda_{max}, \end{cases} \tag{32}$$

where the flux of energy carried by the fast electron stream is given by

$$q_0 = \frac{n_b c^2}{2} (p_{max} + p_{min}).$$

3.3. Maxwellian spectrum

For the 1D Maxwellian spectrum of nonrelativistic fast electrons

$$S(p') = \frac{2}{\pi^{1/2} p_h} \exp \left[- \left(\frac{p'}{p_h} \right)^2 \right],$$

where $p_h = (2kT_h m_e)^{1/2}$ is the momentum corresponding to the temperature of fast electrons T_h, the distribution function is

$$f(x, p) = n_b \frac{2}{\pi^{1/2} p_h} \exp \left[- \left(\frac{p^4}{p_h^4} + \frac{x}{\lambda_h} \right)^{1/2} \right] \times$$

$$\times \left[1 + \left(\frac{p_h}{p} \right)^4 \frac{x}{\lambda_h} \right]^{-1/2}. \tag{33}$$

In expression (33), the stopping length λ_h is introduced for a nonrelativistic fast electron beam with the "thermal" momentum p_h:

$$\lambda_h = \frac{p_h^4}{4g_0 \rho m_e}. \tag{34}$$

According to (5), (17), and (33), the specific heating is determined by the integral

$$W(x) = \frac{q_0}{\lambda_h} \int\limits_0^\infty \exp \left[- \left(u^4 + \frac{x}{\lambda_h} \right)^{1/2} \right] \times$$

$$\times \left(u^4 + \frac{x}{\lambda_h} \right)^{-1/2} u \, du, \tag{35}$$

where $u = p/p_h$ and the flux of energy carried by a Maxwellian nonrelativistic fast electron stream is

$$q_0 = \frac{n_b p_h^3}{2\pi^{1/2} m_e^2}. \tag{36}$$

The approximate calculation gives

$$W(x) \approx \frac{q_0}{\lambda_h} \exp \left[- \left(2\frac{x}{\lambda_h} \right)^{1/2} \right] \tag{37}$$

and then

$$q(x) \approx q_0 \left\{ 1 - \left[1 + \left(2\frac{x}{\lambda_h} \right)^{1/2} \right] \times \right.$$

$$\left. \times \exp \left[- \left(2\frac{x}{\lambda_h} \right)^{1/2} \right] \right\}. \tag{38}$$

For a $1D$ Maxwellian spectrum of ultra-relativistic fast electrons

$$S(p') = p_h^{-1} \exp\left(-\frac{p'}{p_h}\right),$$

the distribution function is

$$f(x, p) = \frac{n_b}{p_h} \exp\left[-\left(\frac{p}{p_h} + \frac{x}{\lambda_h}\right)\right], \qquad (39)$$

where $p_h = T_h/c$. Then the specific heating and transmitted energy by ultra-relativistic Maxwellian fast electron are

$$W(x) = \frac{q_0}{\lambda_h} \exp\left(-\frac{x}{\lambda_h}\right) \qquad (40)$$

and

$$q(x) = q_0 \left[1 - \exp\left(-\frac{x}{\lambda_h}\right)\right]. \qquad (41)$$

Here, the flux of energy carried by an ultra-relativistic Maxwellian fast electron stream is
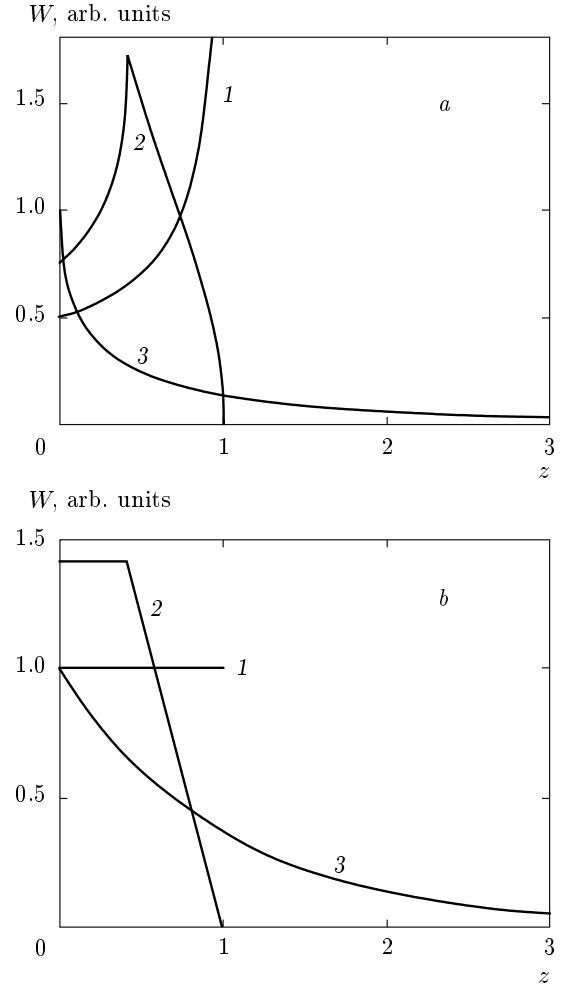
$$q_0 = n_b p_h c^2 \qquad (42)$$

and

$$\lambda_h = \frac{(m_e c)^3 p_h}{g_0 \rho m_e}. \qquad (43)$$

The spatial distributions of the specific heating rate $W(z)$ in a semi-space for nonrelativistic and ultra-relativistic fast electron streams with the above-considered spectra are presented in Fig. 1. The spatial coordinate z is x/λ_0, x/λ_{max}, and x/λ_h in the respective cases of monoenergetic, step-like, and Maxwellian spectra. The function $W(z)$ is normalized to the respective values q_0/λ_0, q_0/λ_{max}, and q_0/λ_h for monoenergetic, step-like, and Maxwellian spectra. The dependences of the heating power $q(z)$ on the plasma thickness for nonrelativistic and ultra-relativistic fast electron streams with the above spectra are presented in Fig. 2. The plasma thickness is normalized to the respective values λ_0, λ_{max}, and λ_h, for monoenergetic, step-like, and Maxwellian spectra. The function $q(z)$ is normalized to the value q_0. For the step-like spectrum, the ratio $p_{min} = 0.8 p_{max}$ was chosen that corresponds to the energy dispersion of 21 % for nonrelativistic fast electrons and 11 % for ultra-relativistic fast electrons. The dependence of specific heating for a monoenergetic spectrum of fast electrons (see curves *1* in Fig. 1) directly reflects the dependence of the stopping power on the distance traveled by a fast electron which, according to (17), is a divergent function for nonrelativistic fast electrons,

$$\frac{dE}{dx} = -\frac{E_0}{2\lambda_0 (1 - x/\lambda_0)^{1/2}}$$

Fig. 1. Spatial distributions of the specific heating rate $W(z)$ in a planar semi-space in the cases of (a) a nonrelativistic and (b) an ultra-relativistic fast electron stream with a monoenergetic spectrum (curve *1*), a step-like spectrum at $0.8 p_{max} \le p \le p_{max}$ (curve *2*), and a Maxwellian spectrum (curve *3*). The spatial coordinate z is x/λ_0, x/λ_{max}, and x/λ_h, in the respective cases of monoenergetic, step-like, and Maxwellian spectra. The function $W(z)$ is normalized to the respective values q_0/λ_0, q_0/λ_{max}, and q_0/λ_h

and, according to (19), is a constant for ultra-relativistic fast electrons.

Hence, the specific heating for a nonrelativistic monoenergetic fast electron stream diverges at the coordinate equal to the stopping length of the fast electron with an initial energy E_0 (see curve *1* in Fig. 1 *a*). The electron energy spread leads to a redistribution of specific heating due to decreasing the stopping with increasing the nonrelativistic fast electron energy. The solutions for a step-like spectrum (see expression
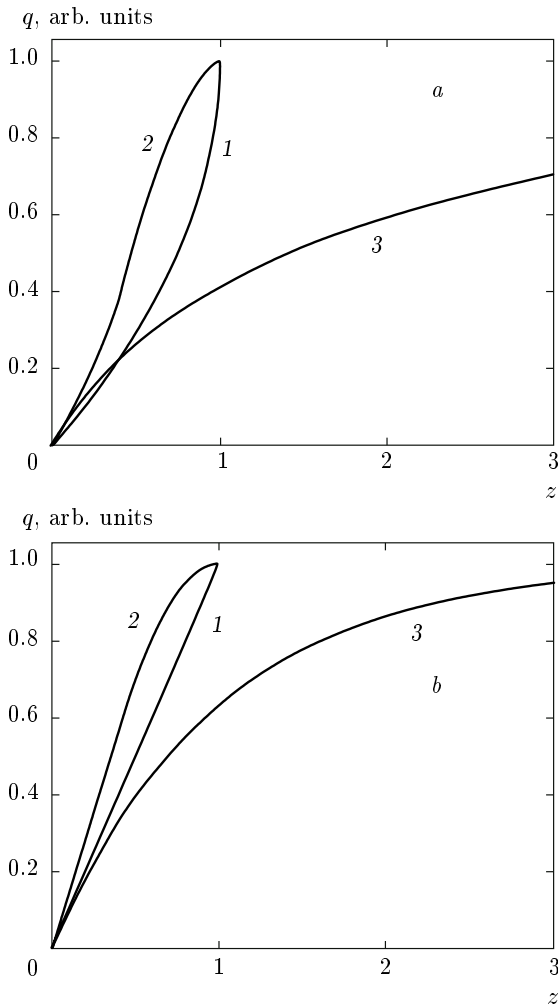
Fig. 2. The dependence of the heating power $q(z)$ on the thickness of a planar layer in the cases of (a) a nonrelativistic and (b) an ultra-relativistic fast electron stream with a monoenergetic spectrum (curve 1), a step-like spectrum at $0.8 p_{max} \leq p \leq p_{max}$ (curve 2), and a Maxwellian spectrum (curve 3). The layer thickness is normalized to the respective values λ_0, λ_{max}, and λ_h in the cases of monoenergetic, step-like, and Maxwellian spectra. The function $q(z)$ is normalized to q_0

(18) and curve 2 in Fig. 1a) and, especially, for the Maxwellian spectrum (see expression (37) and curve 3 in Fig. 1a) clearly show this fact. We note that the distribution of specific heating of a fast electron stream with a step-like spectrum has a maximum in the nonrelativistic case and a kink in the ultra-relativistic case at the coordinate equal to the stopping length of fast electrons with the minimal initial momentum, $x = \lambda_{min}$, and then specific heating monotonically decreases to

0 at the coordinate equal to the stopping length of fast electrons with the maximal momentum, $x = \lambda_{max}$. The specific heating distribution for a Maxwellian fast electron stream is a monotonically decreasing function of the coordinate.

4. PLASMA HEATING AND SHOCK WAVE GENERATION DRIVEN BY LASER-PRODUCED FAST ELECTRONS

Here, we consider applications of the theory of collisional electron transport to the fast ignition and shock wave excitation by a fast electron stream. We consider a Maxwellian spectrum of the heating beam, which is relevant to laser-accelerated fast electrons. A solution for an arbitrary fast-electron temperature can be constructed as an interpolation of the solutions for the specific energy deposition in the nonrelativistic and ultra-relativistic cases.

We approximate the fast electron flux at the boundary q_0 and the fast electron stopping length λ_h as

$$q_0 = \frac{q_{0(nr)}}{1 + \theta}, \qquad \lambda_h = \frac{\lambda_{h(nr)}}{1 + \frac{\pi}{2}\theta^2}, \qquad (44)$$

where $q_{0(nr)}$ and $\lambda_{h(nr)}$ are the energy flow and stopping length of nonrelativistic fast electrons,

$$q_{0(nr)} = \left(\frac{2}{\pi}\right)^{1/2} \frac{n_b (kT_h)^{3/2}}{m_e^{1/2}},$$
$$\lambda_{h(nr)} = \frac{m_e (kT_h)^2}{g_0 \rho}, \qquad (45)$$

and

$$\theta = \left(\frac{2}{\pi} \frac{kT_h}{m_e c^2}\right)^{1/2}. \qquad (46)$$

According (37) and (40) the following interpolations can then be obtained for the temperature and the specific deposited energy distributions in a heated layer:

$$T(x) \approx \frac{T_b}{1 + \theta} \times$$
$$\times \left\{ \exp\left[-\left(2\frac{x}{\lambda_h}\right)^{1/2} \right] + \theta \exp\left(-\frac{x}{\lambda_h}\right) \right\}, \quad (47)$$

$$Q(x) \approx \frac{Q_0}{1 + \theta} \left\{ 1 - \left[1 + \left(2\frac{x}{\lambda_h}\right)^{1/2} \right] \times \right.$$
$$\left. \times \exp\left[-\left(2\frac{x}{\lambda_h}\right)^{1/2} \right] + \theta \left[1 - \exp\left(-\frac{x}{\lambda_h}\right) \right] \right\}, \quad (48)$$

where

$$T_0 = \frac{q_0 t}{\lambda_h C_V \rho}, \qquad Q_0 = q_0 t.$$

In the extreme cases $T \ll mc^2$ and $T \gg mc^2$, solutions (44)–(48) correspond to the respective nonrelativistic and ultra-relativistic cases.

The lowest value of the energy of a fast electron beam corresponds to the heating of a given mass of the DT plasma with the areal density satisfying the ignition criterion $\rho x_{ig} = 0.6 \text{ g/cm}^2$ at the thermonuclear temperature provided by a monoenergetic beam. Estimates for a beam with a Maxwellian spectrum that are available in the literature are based on the averaged stopping length. In the case of an electron beam, this approach leads to the igniting beam energy overestimated by a factor of 1.56 in comparison with the monoenergetic beam [23].

To improve this estimate, we consider the solution of the kinetic equation obtained above. The areal density of the DT plasma $\mu = \rho x_{ig} = 0.6 \text{ g/cm}^2$ corresponds to the stopping range of a relativistic electron with the energy about 0.8 MeV [10, 22]. Hence, to describe the heating of a target by fast electrons, it is necessary to use solution (47), (48) with the parameter θ equal to 1. According to (48), the minimum beam energy required for heating the plasma with a given areal density ρx_{ig} corresponds to the relation $x_{ig}/\lambda_h = 1$. Then the ratio of the igniting beam energies with the Maxwellian ($\theta = 1$) and a monoenergetic spectra, according to (48), is

$$\frac{Q_{Maxw}}{Q_{mono}} = \frac{2}{2 - \left[\left(1 + \sqrt{2}\right) e^{-\sqrt{2}} + e^{-1} \right]} \approx 1.9.$$

Therefore, the Maxwellian spectrum leads to the twofold excess of the igniting beam energy in comparison with the case of a monoenergetic beam.

We now consider the effect of the Maxwellian spectrum on the characteristics of a shock wave driven by a fast electron stream. In [13, 24], an analytic model of a shock wave generation was proposed, where a planar target was heated by a stream of monoenergetic fast electrons. The model is based on a self-similar solution [25] for an isothermal expansion of a given mass of substance determined by the fast electron stopping range. The parameters that determine the shock wave pressure and the time of the pressure formation (loading time) are the fast electron stopping range μ and the velocity of rarefaction wave in the heated material D. The velocity D for a semi-infinite target with a density ρ depends on the intensity of the fast electron flux absorbing in the target region with a mass equal to the fast electron range $m = \mu$ and the initial target density [13, 24]:

$$D = \left(\frac{q}{\rho} \right)^{1/3}. \tag{49}$$

The scale of ablation pressure is proportional to the product ρD^2:

$$P = 0.86 \rho^{1/3} q^{2/3}. \tag{50}$$

The loading time is approximately the time of rarefaction wave propagation through the heated region:

$$t_h = 1.6 \frac{\mu}{\rho^{2/3} q^{1/3}}. \tag{51}$$

Relations (50), (51) were applied in [13, 24] to shock wave generation with a third harmonic of the Nd-laser pulse with the intensity of 1 PW/cm² incident on a planar DT target precompressed to a density of about 10 g/cm³. With a monoenergetic spectrum assumed for nonrelativistic laser-produced fast electrons, it was shown that the fast electron heating under these conditions leads to the generation of a shock wave with the pressure of 700 Mbar during the time of approximately 10 ps. Such a pressure satisfies the shock ignition requirements, according to which the igniting pressure should exceed 300 Mbar during the time of 200–300 ps [26, 27]. The analytic model results are in good agreement with the numerical simulations performed by a hydrokinetic code [13, 24].

Currently, the use of an intense laser pulse is the most effective method for generating powerful shock waves with a pressure of 100 Mbar, which is used in laboratory EOS experiments (see, e. g., review [28]). A beam of laser-accelerated charged particles, in addition to a high-energy density flux, can heat a material with an initial solid density. This is in a contrast with the laser radiation, which is absorbed in the region of the critical plasma density. A higher density in the energy deposition zone makes it possible to achieve a much higher pressure of a shock wave driven by the beams of laser-accelerated electrons or ions in comparison with the laser beam itself. This may be true in spite of a relatively low conversion efficiency of the laser pulse energy into the energy of fast charged particles. Of greatest interest is the use of a laser-accelerated fast electron beam, for which such a conversion efficiency, as mentioned in the Introduction, is substantially higher than for the fast ion beam. It may reach 20–30 %, according to the experimental data.

According to (50), at the monoenergetic fast electron intensity 10 PW/cm², the shock wave pressure, for example, in aluminum can be about 1.2 Gbar, which is more than an order of magnitude greater than the pressure achieved in the current EOS experiments. The scale of laser pulse energy corresponding to a Gbar shock wave generation for EOS experiments is about

10 kJ. This energy value is determined, in particular, by the specific requirements of the shock-wave EOS experiment, which consist in the fact that the shock wave should remain plane and stationary during the measurement period. These requirements impose the constraints on the minimum values of the laser pulse duration and beam radius, which at least should be respectively greater than the loading time and the thickness of the target layer heated by the fast electron beam. We assume that the beam of fast electrons with an intensity of 10 PW/cm² is generated by the third harmonic of Nd-laser radiation with an intensity of 100 PW/cm², which corresponds to the conversion efficiency of the laser energy into the energy of fast electrons of 10 %. According to the scaling in Ref. [29], the average energy of fast electrons in this case is about 25 keV. To calculate the fast electron stopping length, which is a key parameter of the problem, we use the approximation dependences in Refs. [22, 24]. These data are based on quantum-statistical calculations of the Coulomb logarithm in describing the interaction of fast electrons with electrons and ions of dense plasma, obtained in Refs. [30–32]. In particular, these calculations include the effects of reducing the Debye screening radius in strongly coupled plasmas, which lead to logarithmic corrections in increasing the fast electron stopping length. In the considered conditions of Gigabar shock wave generation, when fast electrons heat the plasma with a density of several g/cm³ up to the temperature of several hundred eV, the plasma coupling parameter, which is the ratio of the average values of the potential energy of the plasma electron interaction and its kinetic energy, $\Gamma \approx 5(A\rho)^{1/3}/Z^{1/3}T$ (with the density and temperature measured in g/cm³ and eV) is only 0.01–0.03. Therefore, the coupling plasma correction to the fast-electron stopping length is negligible in this case. When fast electrons heat the plasma with a density of several hundred g/cm³, such a correction can reach 10 % and more. According to Refs. [22, 24], the stopping length of an electron of such an energy in aluminum is about 10 μm. Expression (51) gives the loading time equal to about 45 ps. Then the minimum values of the pulse duration and the beam radius should be chosen equal to 200 ps and 100 μm. At the intensity of 100 PW/cm², the laser pulse energy for generation of a Gbar shock wave satisfying the EOS experiment requirements is about 6 kJ. Using a beam of relativistic electrons corresponding to the target irradiation by a laser pulse with an intensity exceeding 10^{18} W/cm² can provide a pressure even greater than 10 Gbar. However, taking the requirements of the shock-wave EOS experiment into account, the laser pulse energy in this case

must be at least 100 kJ.

In the case of a monoenergetic electron beam, all its energy is spent on the formation of the ablation pressure and excitation of a shock wave, while in the case of a Maxwellian spectrum, only a fraction of that energy can be spent on ablation. High-energy electrons with a Maxwellian spectrum transfer their energy to the region ahead of the shock wave front, thereby producing a heating of the material prior to its compression. A relation between the energies of the two spectral groups of fast electrons responsible for the shock wave generation and preheating processes is the key element for understanding the Maxwellian spectrum effect on the shock wave characteristics. The general relation between the energies of these groups of electrons is deduced from the shock wave generation requirement: $u_{sw} > c_s$, where u_{sw} is the piston (downstream) plasma velocity and c_s is the upstream sound velocity. With the shock wave assumed to be strong, such a criterion determines the coordinate of an ablation boundary x_a as

$$\int_0^{x_a} W^{1/2}dx > (\gamma_a + 1)^{1/2} x_a W^{1/2}|_{x=x_a}. \qquad (52)$$

Substituting solution (37) in expression (52) and integrating, we obtain the equation for the ablation coordinate in the case of nonrelativistic Maxwellian fast electrons

$$\exp\xi_a > \frac{1}{2}(\gamma + 1)^{1/2}\xi_a^2 + \xi_a + 1, \qquad (53)$$

where

$$\xi_a = \left(\frac{x_a}{2\lambda_h}\right)^{1/2}.$$

For $\gamma_a = 5/3$ the requirement in (53) is satisfied at $\xi_a > 1.4$ and, therefore, at $x_a > 4\lambda_h$. Thus, according to (17), the nonrelativistic fast electrons with a Maxwellian spectrum with energies $E < E_a = 2T_h$ are responsible for the generation of a shock wave, including evaporation of the target material and creation of ablation pressure. The fast electrons with energies $E > 2T_h$ are responsible for preheating the material upstream the shock wave front. According to (38), we have

$$\frac{q(x_a)}{q_0} \approx 0.78, \qquad (54)$$

that is, approximately, 78 % of the fast electron stream energy is spent for ablation and 22 % for preheating.

Substituting solution (40) in expression (52) and integrating, we obtain the following equation that determines the ablation coordinate in the case of ultrarelativistic Maxwellian fast electrons:

$$\exp\xi_a > (\gamma + 1)^{1/2}\xi_a + 1, \qquad (55)$$

where

$$\xi_a = \frac{x_a}{2\lambda_h}. \tag{56}$$

With $\gamma_a = 5/3$, requirement (55) is satisfied for $\xi_a > 0.9$ and therefore for $x_a > 1.8\lambda_h$. Thus, according to (19), the ultra-relativistic fast electrons with a Maxwellian spectrum with energies $E < E_a = 1.8T_h$ contribute to the generation of a shock wave, including evaporation of the target material and creation of ablation pressure. The fast electrons with energies $E > 1.8T_h$ contribute to the preheat of a material upstream the shock wave front. According to (41), we have

$$\frac{q(x_a)}{q_0} \approx 0.84. \tag{57}$$

Therefore, in comparison with nonrelativistic fast electrons, the ultra-relativistic fast electrons spend a larger part of their energy for the excitation of shock waves and a smaller part for preheating (84 % and 16 % respectively). Hence, at the same intensities of Maxwellian and monoenergetic beams, the shock wave pressure driven by a Maxwellian beam is smaller than the one driven by a monoenergetic beam. That is due to the reduction in the energy spent on heating the material in the ablation region. According to (51), the pressure amplitude decreases as

$$\frac{P_{Maxw}}{P_{mono}} = \left(\frac{q(x_a)}{q_0}\right)^{2/3}.$$

By itself, the pressure drop is insignificant. According to (54) and (57), the pressure decreases by 1.2 times in the case of nonrelativistic electrons and by 1.1 times in the case of ultra-relativistic electrons. The Maxwellan spectrum effect is much stronger on a spatial and temporal characteristics of the shock wave. As shown above, the thickness of the ablation region x_a in the case of a Maxwellian beam increases by 4 times in the nonrelativistic case and 1.8 times in the ultra-relativistic case in comparison with a monoenergetic beam. Moreover, according to (51), the loading time increases as

$$\frac{t_{h(Maxw)}}{t_{h(mono)}} = \frac{x_{a(Maxw)}}{x_{a(mono)}} \left(\frac{q_0}{q(x_a)}\right)^{1/3}.$$

Thus, the loading time in the case of a Maxwellian beam increases by 4.3 times in the case of nonrelativistic electrons and by 1.9 times in the case of ultra-relativistic electrons in comparison with the case of a monoenergetic beam. These results are in good agreement with numerical calculations [33, 34] of igniting shock waves driven by a beam of nonrelativistic fast electrons with a Maxwellian spectrum.

The effect of the Maxwellian energy distribution is essential. For the igniting shock wave, the effect of increasing the thickness of the ablation region is the most important. It requires a modification of the shock-ignited target design such that the areal density of the precompressed target should be larger by a factor of 4 than the target designed for a monoenergetic igniting beam.

In the case of Gigabar wave generation for EOS studies, both the effects of increasing the ablation region thickness and the loading time are important. For the considered example of a Gigabar shock wave, the Maxwellian spectrum leads to increasing the ablation region thickness and loading time to 40 μm and 80 ps. As a result, choosing the laser pulse duration and beam radius to be equal to 300 ps and 200 μm requires increasing the laser pulse energy from 6 up to 24 kJ in order to generate a shock wave with a pressure of about 1 Gbar for EOS experiments.

5. CONCLUSION

An exact solution of a stationary relativistic kinetic equation for the distribution function of fast electrons with an arbitrary initial spectrum allows finding a simple analytic form of the spatial distribution of the specific energy deposited by a high-energy electron stream in a plane semi-space plasma with an arbitrary density distribution. Broadening the fast electron spectrum leads to increasing the range of energy deposition and to a spatial redistribution of specific heating.

The fast electron spectrum determines the requirements to the energy of fast igniting and shock wave generating beams. The Maxwellian spectrum, which is most appropriate for laser-driven fast electrons, leads to the necessity of a two-fold increase in the relativistic electron beam energy, which is required for fast ignition of an ICF target, in comparison with the case of a monoenergetic beam. The parameters of the shock wave driven by a fast electron stream depend on the fast electron spectrum. Broadening the fast electron spectrum leads to decreasing the ablation pressure and increasing the ablation region thickness as well as the time of ablation pressure formation in comparison with the case of the monoenergetic spectrum. The energy of nonrelativistic fast electrons with the Maxwellian spectrum is separated into two fractions, one of which, approximately 78 % of the total energy, is spent to the shock wave excitation and the rest fraction of 22 % of total energy is spent for preheating the material ahead of shock front. It leads to a not so large decrease in the ablation pressure by a factor of 1.2, but to a significant increase in the time of shock wave generation

by a factor 4.3. The most important consequence of the Maxwellian spectrum of fast electrons for the design of a shock ignition target is the increase in the fast electron energy deposition range in comparison with a monoenergetic beam. The design of the target must provide such a regime of target precompression that the peripheral part of precompressed material should have a mass larger by a factor of 4 than the range of fast electrons with the energy equal to the temperature of the Maxwellian distribution.

The most important consequence of the Maxwellian fast electron spectrum for the characteristics of Gbar shock waves designed for EOS experiments deals with both the effects of increase in the fast electron energy deposition range and the time of ablation pressure formation in comparison with the case of a monoenergetic beam. The laser pulse energy needed to generate such a wave in the case of a Maxwellian spectrum beam increases by 4 times in comparison with the case of a monoenergetic beam, from 6 up to 24 kJ.

REFERENCES

1. J. P. Freidberg, R. W. Mitchel, R. L. Morse et al., Phys. Rev. Lett. **28**, 795 (1972).

2. M. Brunel, Phys. Rev. Lett. **59**, 52 (1987).

3. W. L. Kruer and K. Estabrook, Phys. Fluids **28**, 430 (1985).

4. V. Yu. Bychenkov and V. T. Tikhonchuk, in book: *Nuclear Fusion by Inertial Confinement*, ed. by G. Velarde et al., CRC Press (1993).

5. G. Mourou, T. Tajima, and S. Bulanov, Rev. Mod. Phys. **78**, 3092006 (2006).

6. V. S. Belyaev, V. P. Krainov, V. S. Lisitsa, and A. P. Matafonov, Uspekhi Fiz. Nauk **178**, 823 (2008).

7. S. Yu. Gus'kov, S. Borodziuk, M. Kalal et al., Quant. Electr. **34**, 989 (2004).

8. S. Yu. Gus'kov, A. Kasperczyk, T. Pisarczyk et al., Quant. Electr. **36**, 429 (2006).

9. N. G. Basov, S. Yu. Gus'kov, and L. P. Feoktistov, J. Sov. Laser Res. **13**, 396 (1992).

10. M. Tabak, J. M. Hammer, M. E. Glinsky et al., Phys. Plasmas **1**, 1626 (1994).

11. V. A. Scherbakov, Sov. J. Plasma Phys. **9**, 240 (1983).

12. R. Betti, C. D. Zhou, K. S. Anderson et al., Phys. Rev. Lett. **98**, 155001 (2007).

13. S. Yu. Gus'kov, X. Ribeyre, M. Touati et al., Phys. Rev. Lett. **109**, 255004 (2012).

14. J. J. Duderstadt and G. A. Mozes, *Inertial Confinement Fusion*, J. Wiley and Sons, New York (1982).

15. S. Atzeni and J. Meyer-ter-Vehn, *The Physics of Inertial Fusion*, Oxford Univ. Press, Oxford (2004).

16. G. H. McCall, R. Kopp, T. H. Tan et al., Plasma Phys. **25**, 237 (1983).

17. T. H. Tan, G. H. McCall, R. Kopp et al., Phys. Fluids **24**, 754 (1983).

18. S. Yu. Gus'kov, V. V. Zverev, and V. B. Rozanov, Sov. J. Quant. Electr. **13**, 498 (1983).

19. P. P. Volosevich and V. B. Rozanov, JETP Lett. **33**, 17 (1981).

20. S. Yu. Gus'kov and V. V. Zverev, in book: *The Theory of Target Compression by Longwave Laser Emission*, ed. by G. V. Sklizkov, Nova Sci. Publ. (1987).

21. R. J. Harrach and R. E. Kidder, Phys. Rev. A **23**, 887 (1981).

22. S. Atzeni, A. Schiavi, J. J. Honrubia et al., Phys. Plasmas **15**, 056311 (2008).

23. S. Yu. Gus'kov, Plasma Phys. Rep. **39**, 3 (2013).

24. X. Ribeyre, S. Yu. Gus'kov, M. Touati et al., Phys. Plasmas **20**, 062705 (2013).

25. V. S. Imshennik, Sov. Phys. Doklady **5**, 263 (1960).

26. L. J. Perkins, R. Betti, K. N. Lafortune et al., Phys. Rev. Lett. **103**, 045004 (2009).

27. X. Ribeyre, M. Lafon, G. Schurtz et al., Plasma Phys. Control. Fusion **51**, 124030 (2009).

28. S. G. Garanin, Uspekhi Fiz. Nauk **181**, 434 (2011).

29. A. R. Bell, J. R. Davies, S. Guerin, and H. Ruhl, Plasma Phys. Control. Fusion **39**, 653 (1997).

30. C. K. Li and R. D. Petrasso, Phys. Plasmas **13**, 056314 (2008).

31. A. A. Solodov and R. Betti, Phys. Plasmas **15**, 042707 (2008).

32. M. Storm, A. A. Solodov, J. F. Myatt et al., Phys. Rev. Lett. **102**, 235004 (2009).

33. T. E. Fox, A. P. L. Robinson, and J. Pasley, Phys. Plasmas **20**, 122707 (2013).

34. Ph. Nicolai, J.-L. Feugeas, M. Touati, X. Ribeyre, S. Gus'kov, and V. Tikhonchuk, Phys. Rev. E **89**, 033107 (2014).